

See discussions, stats, and author profiles for this publication at: <https://www.researchgate.net/publication/24348963>

Effect of Surface Charge on Colloidal Charge Reversal

ARTICLE in THE JOURNAL OF PHYSICAL CHEMISTRY B · MAY 2009

Impact Factor: 3.3 · DOI: 10.1021/jp900959y · Source: PubMed

CITATIONS

22

READS

28

4 AUTHORS, INCLUDING:



[Alberto Martin-Molina](#)

University of Granada

52 PUBLICATIONS 945 CITATIONS

SEE PROFILE



[César Rodríguez-Beas](#)

Universidad de Sonora (Unison)

6 PUBLICATIONS 111 CITATIONS

SEE PROFILE



[Roque Hidalgo-Alvarez](#)

University of Granada

265 PUBLICATIONS 4,224 CITATIONS

SEE PROFILE

Effect of Surface Charge on Colloidal Charge Reversal

A. Martín-Molina,^{*,†} C. Rodríguez-Beas,[†] R. Hidalgo-Álvarez,[†] and M. Quesada-Pérez[‡]

Grupo de Física de Fluidos y Biocoloides, Facultad de Ciencias, Universidad de Granada, Campus de Fuentenueva, sn, 18071, Granada, Spain, and Departamento de Física, Escuela Politécnica Superior de Linares, Universidad de Jaén, 23700 Linares, Jaén, Spain

Received: February 2, 2009; Revised Manuscript Received: April 3, 2009

The objective of this research work is to understand the effect of the surface charge density on the charge reversal phenomenon. To this end, we use experimental results and computer simulations. In particular, we measure the electrophoretic mobility of latex particles (macroions) in the presence of a multivalent electrolyte. We have focused on the electrolyte concentration range at which a reversal in the electrophoretic mobility is expected to happen. In particular, the role of the surface charge on the charge reversal process is looked into from several latexes with the same functional group but different surface charge densities. Although the mechanism responsible for the colloidal charge reversal is still a controversial issue, it is proved that ionic correlations are behind the appearance of such phenomenon (especially near the macroion surface). This conclusion can be inferred from a great variety of theoretical models. According to them, one of the factors that determine the charge reversal is the surface charge density of the macroions. However, this feature has been rarely analyzed in experiments. Our results appear therefore as a demanded survey to test the validity of the theoretical predictions. Moreover, we have also performed Monte Carlo simulations that take the ion size into account. The correlation found between experiments and simulations is fairly good. The combination of these techniques provides new insight into the colloidal charge reversal phenomena showing the effect of surface charge.

Introduction

Although considerable effort has been done in the past decades with the aim of comprehending how ions adsorb onto charged interfaces, the mechanism of such ion *condensation* is still under investigation.^{1–4} The resulting structure of ions around a charged macroion is termed electric double layer (EDL). Obviously, this ionic distribution plays an important role in the stability and electrokinetic of electrostatically stabilized colloidal dispersions. This is the case, for instance, of DNA molecules dispersed in biological solutions. The basic model of planar EDL was developed by Gouy and Chapman (GC) more than 90 years ago. This classical model is in turn based on the Poisson–Boltzmann (PB) equation, which neglects the ion size. According to the GC model, the colloidal particles are smooth and uniformly charged planes immersed in a dielectric continuum composed of mobile ions. Although this rudimentary description of a double layer is a very simple model to represent any real colloidal system, it may be reasonable when the electrolyte (mostly monovalent) concentration and the surface charge are low enough. However, the model fails if these conditions do not hold. For instance, in the presence of multivalent electrolyte, the colloid charge can become overcompensated and its effective charge is reverted. This phenomenon is called *charge reversal* (CR). Although in the literature the term charge reversal is also called *overcharging* or *charge inversion*,^{3–5} some authors have recently defined these concepts elucidating the differences between them.⁶ Accordingly, we will use the term charge

reversal in this work. From a theoretical point of view, the PB equation is not able to predict CR if the so-called *specific interactions* are not considered. On the contrary, a vast number of theories such as integral equations,^{3,6–10} field-theoretic approaches,^{11,12} and one-component plasma models (OCP)^{1,2,13} have been put forward to describe this effect. All these theories have in common that they consider the correlations between ions as the responsible of the CR. Accordingly, this phenomenon is expected to occur for highly charged macroions in the presence of multivalent ions. This feature is also predicted by computer simulations, which are frequently used to study the validity of the theoretical models.^{14–28} In contrast to the enormous theoretical and simulations research works, CR has been scarcely studied from an experimental viewpoint. The lack of experimental studies is generally due to the technical difficulties found in dispersions with high concentrations of multivalent ions. Nevertheless, CR can be studied by means of electrophoresis experiments, where a reversal in the electrophoretic mobility (μ_e) is reported for charged colloids in a solution that contained multivalent ions.^{29–38} AFM experiments performed by Besteman et al. have also provided very interesting results of CR,^{39–41} and the survey on the different origins of charge inversion for phospholipids performed by Vaknin et al.^{42,43} must be mentioned as well.

Although some technical aspects make it difficult to perform systematic studies of CR (as stated above), the effect of the surface charge density on CR has already been previously studied in a preliminary paper.³¹ However, the experimental systems employed therein were diverse types of latexes, whose charge depended on the pH because their functional groups were weak acids. Given that some authors claim that the CR process occurring in these kind of systems can be due to chemical interactions between ions and the macroion surface

* To whom correspondence should be addressed at Departamento de Física Aplicada, Facultad de Ciencias, Universidad de Granada, Campus de Fuentenueva, sn, 18071, Granada, Spain. E-mail: almartin@ugr.es. Phone: 0034958240025. Fax: 0034958243214.

[†] Universidad de Granada.

[‡] Universidad de Jaén.

groups (i.e., *specific adsorption*),²⁹ CR could not be unequivocally attributed to ion correlations appearing at high surface charge densities and neglected by the PB approach. In order to overcome this deficiency, we intend to study several latexes with the same strong acid surface groups but different surface charge density. Thus, differences in the mobility reversal of these systems can be clearly attributed to changes in ionic correlations with varying the surface charge density. Furthermore, in the previous work, the experimental data were analyzed with the integral equation theory termed hypernetted-chain/mean spherical approximation (HNC/MSA). However, Monte Carlo (MC) simulations have recently proved that the HNC/MSA theory can fail in the description of experimental data at high multivalent electrolyte concentration and/or high surface charge density,^{21,24,38} which might lead to imprecise conclusions. Accordingly, our new experimental results are compared with MC simulations rather than with such theoretical predictions. In short, two aspects of the previous work on the surface charge effect are therefore improved in this survey: (i) the experimental systems (replacing weak-acid latexes by a set of strong-acid latexes with different surface charge densities); and (ii) the theoretical description of the electric double layer (replacing the integral equation approach by MC computations). The remainder of the work is organized as follows. In the next section, some technical details of simulations are outlined. Next, the samples used for this study and the experimental technique are presented. Subsequently, the results are shown and discussed and some conclusions are finally highlighted.

Theoretical Background

In the MC simulations performed in this work, the planar EDL is described by a primitive model (PM) of electrolyte in which the plane wall is assumed to be smooth and uniformly charged whereas the ions are treated as charged hard spheres immersed in a dielectric continuum. The calculations have been carried out by using the Metropolis algorithm applied to a canonical ensemble for a collection of N ions confined in a rectangular prism (or cell) of dimensions $W \times W \times L$. The impenetrable charged wall is located at $z = 0$ whereas at $z = L$ another impenetrable wall without charge is placed and periodic boundary conditions were used in the lateral directions (x and y). The cell contains the ionic mixture corresponding to the bulk electrolyte solution together with an excess of counterions neutralizing the surface charge. The interaction energy between mobile ions is given by

$$u(\vec{r}_{ij}) = \frac{Z_i Z_j e^2}{4\pi\epsilon_0\epsilon_r r_{ij}} \quad r_{ij} > d$$

$$u(\vec{r}_{ij}) = \infty \quad r_{ij} < d$$
(1)

where d is the hydrated ion diameter, Z_i is the valence of ion i , e is the elementary charge, ϵ_0 is the permittivity of free space, $\epsilon_r (=78.5)$ the relative permittivity of the solvent (corresponding to water at a temperature of 298 K), $|\vec{r}_{ij}|$ is the relative position vector and $r_{ij} = |\vec{r}_{ij}|$ is the distance between ions i and j , whereas the interaction energy of ion i with the charged wall is

$$u(\vec{r}_i) = -\frac{\sigma_0 Z_i e z_i}{2\epsilon_0\epsilon_r} \quad (2)$$

where z_i is the z -coordinate of particle i and σ_0 is the surface charge density of the charged wall.

The number of ions in each simulation was fixed, checking that the cell size was always large enough. Likewise, the systems

were always thermalized before collecting data for averaging and the acceptance ratio was kept between 0.4 and 0.6.

Due to the long range of the electrostatic interactions, the energy must be evaluated very carefully. In these simulations, we have applied the so-called *external potential method* (EPM), in which each mobile ion is allowed to interact with the others in the MC cell according to the usual minimum image convention.^{14,15,44} The remaining part (all charges outside the cell) is considered in the evaluation energy through an external potential, $\psi_{\text{ext}}(z)$. This function is calculated assuming that the ionic distribution profiles outside the cell are identical to those inside. Thus, the external potential must be updated during the simulation using the current ion profiles and is given by

$$\psi_{\text{ext}}(z) = \frac{1}{4\pi\epsilon_0\epsilon_r} \int_0^L \int_{\pm W/2}^{\pm\infty} \int_{\pm W/2}^{\pm\infty} \frac{\rho(z')}{\sqrt{(x')^2 + (y')^2 + (z' - z)^2}} dx' dy' dz' \quad (3)$$

where $\rho(z')$ is the charge density at z' (both outside and inside the cell). The integration over x' and y' can be performed analytically, whereas the integration over z' must be carried out numerically since the function $\rho(z')$ is tabulated. This is equivalent to considering the electrostatic potential generated by a set of infinite sheets of thickness dz' and surface charge density $\rho(z')dz'$ from which the central square “hole” (of dimensions $W \times W$) is removed. The electrostatic potential of an *entire* infinite sheet can be calculated as in eq 5, whereas the electrostatic potential of the square hole removed from its center, which must be subtracted, can be calculated using the integral appearing in eq 16 of ref 44. In a previous work,²¹ the energy was also calculated by following an alternative method to the EPM, originally developed by Lekner for systems with 2D symmetries that has recently been improved by Sperb.^{45,46} However, no significant differences were found in comparing with the EPM.

Having computed the local ion concentrations, the diffuse potential can be calculated from

$$\psi_d \equiv \psi(a) = \frac{e}{\epsilon_r \epsilon_0} \int_a^\infty (a - z) \sum_j Z_j \rho_j(z) dz \quad (4)$$

where $a = d/2$ is the hydrated ion radius and $\rho_j(z)$ is the local density of j ions at a distance z from the charged surface ($j = 1, 2$ for counterions and co-ions, respectively). The integral appearing in eq 4 should be evaluated over an infinite interval, but this is not feasible in practice because computer simulations are always carried out in a box with a finite length (L). In order to take this aspect into account, it is usual to choose a cutoff distance (L_c) admitting that, theoretically, the contribution to such an integral is negligible (for $z > L_c$) if $\sum_{j=1,2} Z_j \rho_j(z) = 0$. This is the condition of local electroneutrality, which can always be fulfilled far enough from the charged surface (in the solution bulk). Due to the term $(a - z)$, however, the fluctuations of $\sum_{j=1,2} Z_j \rho_j(z)$ (computed from simulations) could be considerably amplified, contributing appreciably to the integral of eq 7. To avoid this undesirable contribution L_c must not be too large. In our runs, we took $L_c = 0.5L$, and chose values for L trying to guarantee the electroneutrality condition at $0.5L$. The diffuse potential and its statistical error were computed by collecting many averages of ψ_d (according to eq 7) during the runs.

Experimental Section

As mentioned before, this research work is focused in the study of similar latexes that only differ in the surface charge density. The main properties of the systems are displayed in

TABLE 1: Particle Diameter and Surface Charge Density of the Latexes

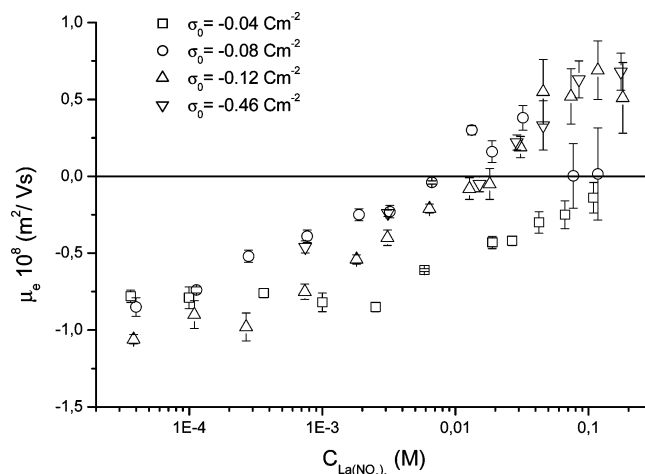
latex	diameter (nm)	σ_0 (C m ⁻²)
L1	186 ± 6	-0.04
L2	85 ± 1	-0.08
L3	507 ± 5	-0.12
L4	505 ± 6	-0.46

Table 1. The first two systems (L1 and L2) were prepared by a two stage “shot growth” emulsion polymerization process in absence of emulsifiers and subsequently, accordingly two styrene/sodium styrene sulfonate copolymers were obtained. The details of synthesis method are described in ref 47. In order to study similar systems with different surface charge, two other sulfonate latexes (L3 and L4) were provided by Ikerlat Polymers S.L. Table 1 shows the diameter and surface charge density of the latexes. The particle sizes were obtained by photon correlation spectroscopy (PCS) whereas conductometric and potentiometric titrations were used to determine the surface charge density. These experiments were performed with Crison instruments (pH-meter and conductimeter), at 25 °C in a stirred vessel flushed with nitrogen. Titration agents were NaOH and HCl (these titration techniques are illustrated in refs 31, 32, and 48). As can be seen, the four latexes present different particle size and well-differentiated values of σ_0 , ranging from -0.04 C m⁻² (L1) to -0.46 C m⁻² (L4). Previous experiments show that differences in the particle size such as those found in these systems do not involve changes in the electrophoresis data. In contrast, differences in the surface charge allows us to study its effect in the electrophoretic behavior within one order of magnitude. In particular, μ_e is measured as a function of $\text{La}(\text{NO}_3)_3$. According to previous studies, this multivalent electrolyte enhances the CR process for salt concentrations that can be used straightforward in our electrophoresis experiments.^{33–36,38}

The electrophoretic mobility measurements were performed by using a ZetaPALS instrument (Brookhaven, USA), which is based on the principles of phase analysis light scattering (PALS). The setup is especially useful at high ionic strengths and nonpolar media, where mobilities are usually low. The PALS is able to measure values of μ_e at least two orders of magnitude lower than traditional light-scattering methods based on the shifted frequency spectrum (spectral analysis). Both techniques have in common the analysis of a mixing of scattered light from a suspension of colloidal particles moving in an electric field, with light directly from the source (reference beam light). The frequency of the scattered light is shifted by the Doppler effect and its superposition with the *unshifted* reference one leads to a beating at a frequency that depends on the speed of the particles. The problem arises when the particle velocity is low. For those cases, spectral analysis is not able to generate a complete cycle of the detected signal. However, phase analysis takes place over many cycles of the respective waveforms since the optical phase of the scattered light is characterized by means of the so-called the *amplitude-weighted phase difference* (AWPD) function instead of a simple correlation treatment. This function improves the statistic behavior because the detected signal fluctuates in amplitude due to the relative movements of particles and concentration fluctuations. For a complete discussion of the PALS method and AWPD treatment, we refer the reader to refs 49 and 50.

Results and Discussion

In order to study the effect of charge, let us first evaluate the electrophoretic mobility for the four different latexes as a

**Figure 1.** Experimental results: Electrophoretic mobility as a function of the concentration of $\text{La}(\text{NO}_3)_3$ for the four latexes shown in Table 1.

function of the salt concentration. In this way, changes in the electrokinetic behavior of the systems will be univocally related to differences of the surface charge densities. In particular, figure 1 shows μ_e as a function of the concentration of $\text{La}(\text{NO}_3)_3$. The most remarkable feature in these data is that CR is observed only for the two most charged latexes (L3 and L4). Before discussing this experimental finding in detail, let us outline some general aspects found in the figure. As can be seen, we may distinguish four features of the electrophoretic mobility as a function of electrolyte concentration: (i) For salt concentrations smaller than 0.02 M, the magnitude of μ_e decreases (in all cases) as the electrolyte concentration increases. (ii) Above 0.02 M, latexes L3 and L4 present mobility reversal, whereas the electrophoretic mobility measured for latexes L1 and L2 tends to be zero at high salt concentrations. (iii) The latex of the greatest surface charge density, $\sigma_0 = -0.46$ C m⁻², has an electrokinetic behavior quite similar to that found for $\sigma_0 = -0.12$ C m⁻². (iv) Once the reversal is reached, the inverted electrophoretic mobility seems to reach a saturation value.

From the two former observations, it is clearly deduced that the occurrence of CR depends fundamentally on the surface charge density. Only when the σ_0 is large enough (-0.12 C m⁻², in this case) the sign of the mobility changes and remains positive. At this point it should be stressed that we admit that a mobility reversal is reached when all the measures at high salt concentrations exhibit a clear reversal in their sign. This criterion is used to distinguish from those cases, such as latex L2, where positive and negatives values of μ_e are observed. In general, alternating values (positive and negative) in the mobility indicates that the system is not stable under these conditions.

Accordingly, the fact that a clear CR is only found for elevated values of σ_0 and for high concentrations of $\text{La}(\text{NO}_3)_3$ implies that only the most charged systems could be electrostatically stabilized under this situation. This feature is apparently logical from a classical point of view: the more surface charge, the more stable system. However, the surprising point is that under these conditions, the more charged systems are stable as a consequence of an effective surface charge that is positive. This aspect is not considered in the framework of classical EDL theories where an increase of the ionic strength always results in electrostatic destabilization. Accordingly, our results suggest that colloidal systems with elevated surface charge densities can be electrically stabilized by the presence of high concentrations of multivalent electrolytes. When this situation occurs, the role

of counterions and co-ions are exchanged as compared to their role at low salt concentration. This feature is predicted by many theoretical models as well as simulations, where the ionic profiles calculated exhibit nonmonotonic behaviors (see for instance Figures 10–12 in ref 21). Therein, CR is justified in terms of ion–ion correlations, which become more important as the colloidal surface charge, valence, and concentrations of counterions increase. As can be seen, such predictions are confirmed by our experiments. Furthermore, our measurements are also consistent with the theoretical predictions obtained by Pianegonda et al.¹³ as well as with the simulations of Diehl and Levin.^{51,52} In their OCP theory, the former proved that the CR can take place if σ_0 is larger than a critical surface charge density (σ_c).¹³ This feature is also predicted by MC simulations performed by Diehl and Levin. These authors calculated the ζ -potential as a function of σ_0 for a high concentration of 3:1 electrolyte (with and without 1:1 salt) in order to predict σ_c .^{51,52} Moreover, in their most recent work, the authors show how σ_c strongly depends on the ionic size and on the electrolyte concentration of multivalent electrolyte. Although their results qualitatively agree with our experiments, there are slight quantitative discrepancies. For instance, they predict that a reversal in the ζ -potential for surface charge densities larger than 0.05 C m^{-2} when the 3:1 salt concentration is 0.1 M (see Figure 1 in ref 52). A similar value for σ_c is predicted by the OCP theory of Pianegonda et al.¹³ However, according to our results, the mobility reversal is not expected to happen under these conditions. We think that there are two explanations for such apparent disagreement. On one hand, Diehl and Levin calculated the ζ -potential at a distance of one ionic diameter from the surface (instead of an ionic radius). On the other hand, the ion size used in their simulations was 0.3 nm whereas in the case of Pianegonda et al. the ion diameter was 0.4 nm . In both cases, the ion size is smaller than that expected for hydrated trivalent cations.^{53,54} Accordingly, if these parameters (distance at which ζ -potential is calculated and the ion size) are modified, the agreement with our electrophoretic measurements could enhance.

Concerning the third aspect previously summarized, above $\sigma_0 = -0.12 \text{ C m}^{-2}$ no differences are appreciated in systems more charged. This finding is also predicted by recent EDL theories and simulations. For instance, MC simulations and the HNC/MSA predict this saturation effect in the electrokinetic potential as the surface charge density increases. Moreover, in some cases, the potential decreases when the surface charge is large enough (see Figure 14 in ref 21). Consequently, the data shown in Figure 1 provide an experimental confirmation of some of the most relevant findings predicted theoretically.

In relation to the fourth characteristic of Figure 1, the idea of saturation in the CR is experimentally confirmed. Although this experimental feature had been previously reported by electrophoresis, it is still a controversial issue given that some theoretical approaches do not predict such saturation effect.³⁸

To deepen the understanding of the effect of the surface charge effect in the occurrence of CR, we have used MC simulations to calculate the diffuse potential as a function of the electrolyte concentration for several values of σ_0 . The diffuse potential is intimately related to the ζ -potential, which is an essential quantity to characterize electrokinetic phenomena. In general, the conversion of the electrophoretic mobility into ζ -potential for colloidal particles is not a trivial matter because it involves a rather complex hydrodynamical problem. However, if the electrokinetic radius is large enough, the ζ -potential can

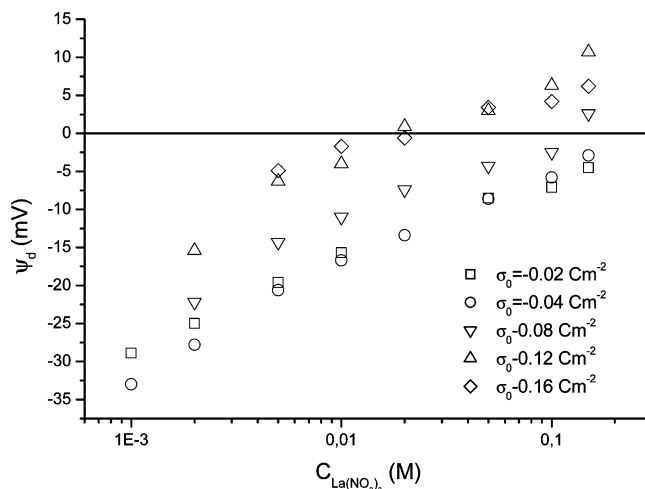


Figure 2. Diffuse potential calculated by MC simulations as a function of the concentration of 3:1 electrolyte for five different values of σ_0 . A value of $d = 0.90 \text{ nm}$ was chosen for the calculations.

be straightforwardly obtained from the Helmholtz–Smoluchowski (HS) approximation:

$$\mu_e = \frac{\varepsilon_0 \varepsilon_r \zeta}{\eta} \quad (5)$$

where η is the viscosity. The electrokinetic potential is often equated to the diffuse potential ($\zeta = \psi_d$). The most compelling argument for making this choice is the experimental evidence that colloidal interaction correlate well with theories if the diffuse layer is chosen as the characterizing parameter.^{55,56} Accordingly, under our experimental conditions we can assume that there is a lineal relationship between μ_e and ψ_d (i.e., eq 5).

Concerning the widely known approximation $\zeta \approx \psi_d$, it should also be mentioned that it is equivalent to assuming that the shear plane is located at one ionic radius from the surface. However, as commented above, Diehl and Levin suggest that the shear plane should rather be located at one ionic diameter.⁵¹ This innovative idea presents two advantages (as compared to classical location of the shear plane): (i) it takes the thermal fluctuations into account; (ii) it overcomes the problems derived from the strong variation of the mean electrostatic potential over a length of one ionic diameter. However, the authors of this paper also admit that this definition is far from intuitive and should be checked by more detailed molecular dynamics simulations, including the explicit solvent.

Figure 2 shows the diffuse potential as a function of the concentration of $\text{La}(\text{NO}_3)_3$ for values of σ_0 in the range -0.02 to -0.16 C m^{-2} . As in previous works, an ion diameter of 0.90 nm obtained from the literature was chosen in the calculations for all the species.^{53,54} As can be seen, the behavior of ψ_d is quite similar to that found for μ_e in Figure 1. A clear reversal is observed for σ_0 larger than -0.12 C m^{-2} (in magnitude). Moreover, the electrolyte concentrations at which $\psi_d = 0$ and $\mu_e = 0$ are practically the same. In both cases it takes places at a concentration of $\text{La}(\text{NO}_3)_3 = 0.02 \text{ M}$. In general, the experimental findings obtained from Figure 1, are confirmed by the simulations. Even the ambiguous behavior found for the latex L2 is corroborated by the simulations. In Figure 1, it can be seen how this latex seems to undergo a mobility reversal but μ_e remains around zero above 0.02 M . This feature is qualitatively captured by simulations in Figure 2, where we can see how a very slight reversal for the highest salt concentration in the case of $\sigma_0 = -0.08 \text{ C m}^{-2}$.

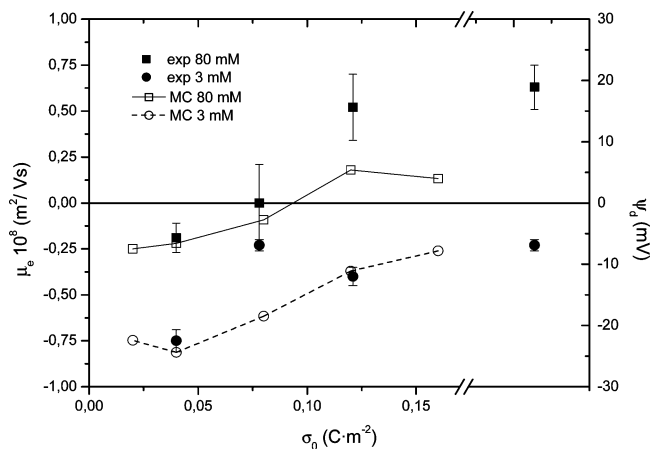


Figure 3. Comparison between experiments and simulations for two particular cases: low and high 3:1 salt concentrations. Symbols stand for μ_e measurements (solid circles and squares for 3 and 80 mM, respectively) whereas lines with symbols correspond to diffuse potentials predicted by simulations (open circles and squares for 3 and 80 mM, respectively).

In order to improve the comparison between Figures 1 and 2, a double y-graph is shown in Figure 3. Herein, we have selected two opposite situations in relation to the reversal point. In particular, we have plotted both the electrophoretic mobility (left axis) and diffuse potential (right axis) as a function of the surface charge density for two electrolyte concentrations. On one hand, we have chosen a low salt concentration of 0.003 M at which CR never takes place. On the other, the situation at $\text{La}(\text{NO}_3)_3 = 0.08 \text{ M}$ is also shown. In this case, a CR clearly occurs for high surface charge densities. From this figure, significant features can be deduced. First, the diffuse potential calculated by MC simulations and electrophoretic mobility experimentally measured exhibit a similar behavior as a function of the surface charge density. Also, these results confirm the fact that CR is propitiated when the multivalent electrolyte concentration and the surface charge density are large enough. Finally, the results also confirm that the CR reaches a saturation value for elevated salt concentration and high surface charge densities. These findings are very important toward the understanding of CR and provide an original quantification of the role played by the surface charge.

Conclusions

We have investigated the role of the surface charge density in the colloidal charge reversal by a double experimental and simulation study that provides unique insight into this phenomenon. In particular, we have studied four latexes of similar functional groups, but different surface charge densities. Furthermore, a model of EDL based on a PM of electrolyte has been analyzed by MC simulations. Accordingly, we have studied the variation of the experimental mobility and the diffuse potential calculated from simulations, as a function of $\text{La}(\text{NO}_3)_3$ concentration. In both cases we have found similar tendencies. The CR is reached for σ_0 above 0.12 C m^{-2} and electrolyte concentrations larger than 0.02 M . This finding corroborates some of the theoretical predictions addressed by sophisticated EDL models that have not been properly tested from an experimental point of view. In this sense, our experiments and simulations also confirm that once CR takes place, it saturates. In other words, values of μ_e and ψ_d reach a saturation situation when the surface charge density and multivalent electrolyte concentration are large enough.

Acknowledgment. The authors are grateful to “Ministerio de Educación y Ciencia, Plan Nacional de Investigación, Desarrollo e Innovación Tecnológica (I+D+i)”, Project MAT2006-12918-C05-01 and -02, “Consejería de Innovación, Ciencia y Empresa de la Junta de Andalucía”, Projects P07-FQM-02496 and P07-FQM-02517, as well as the European Regional Development Fund (ERDF) for financial support. A.M.-M. also thanks the “Programa Ramón y Cajal, 2005, Ministerio de Educación y Ciencia-Fondo Social Europeo (RYC-2005-000829)”. C.R.-B. also thanks to CONACYT (Mexico) for his scholarship.

References and Notes

- (1) Levin, Y. *Rep. Prog. Phys.* **2002**, *65*, 1577.
- (2) Grosberg, A. Y.; Nguyen, T. T.; Shklovskii, B. I. *Rev. Modern Phys.* **2002**, *74*, 329.
- (3) Quesada-Pérez, M.; González-Tovar, E.; Martín-Molina, A.; Lozada-Cassou, M.; Hidalgo-Álvarez, R. *ChemPhysChem* **2003**, *4*, 234.
- (4) Lyklema, J. *Colloids Surf. A* **2006**, *291*, 3.
- (5) Lenz, O.; Holm, C. *Eur. Phys. J. E* **2008**, *26*, 191.
- (6) Jiménez-Ángeles, F.; Lozada-Cassou, M. *J. Phys. Chem. B* **2004**, *108*, 7286.
- (7) Lozada-Cassou, M.; Saavedra-Barrera, R.; Henderson, D. *J. Chem. Phys.* **1982**, *77*, 5150.
- (8) González-Tovar, E.; Lozada-Cassou, M. *J. Phys. Chem.* **1989**, *93*, 3761.
- (9) Kjellander, R. *Ber. Bunsenges. Phys. Chem.* **1996**, *100*, 894.
- (10) Greberg, H.; Kjellander, R. *J. Chem. Phys.* **1998**, *108*, 2940.
- (11) Netz, R. R.; Orland, H. *Eur. Phys. J. E* **2000**, *1*, 67.
- (12) Moreira, A. G.; Netz, R. R. *Eur. Phys. J. E* **2002**, *8*, 33.
- (13) Pianegonda, S.; Barbosa, M. C.; Levin, Y. *Europhys. Lett.* **2005**, *71*, 831.
- (14) van Megen, W.; Snook, I. *J. Chem. Phys.* **1980**, *73*, 4656.
- (15) Torrie, G. M.; Valleau, J. P. *J. Chem. Phys.* **1982**, *86*, 3251.
- (16) Mier-y-Teran, L.; Suh, S. H.; White, H. S.; Davis, H. T. *J. Chem. Phys.* **1990**, *92*, 5087.
- (17) Degève, L.; Lozada-Cassou, M.; Sánchez, E.; González-Tovar, E. *J. Chem. Phys.* **1993**, *98*, 8905.
- (18) Boda, D.; Fawcett, W. R.; Henderson, D.; Sokolowski, S. *J. Chem. Phys.* **2002**, *116*, 7170.
- (19) Bhuiyan, B.; Outhwaite, C. W. *Phys. Chem. Chem. Phys.* **2004**, *6*, 3467.
- (20) Valiskó, M.; Henderson, D.; Boda, D. *J. Phys. Chem. B* **2004**, *108*, 16548.
- (21) Quesada-Pérez, M.; Martín-Molina, A.; Hidalgo-Álvarez, R. *J. Chem. Phys.* **2004**, *121*, 8618.
- (22) Quesada-Pérez, M.; Martín-Molina, A.; Hidalgo-Álvarez, R. *Langmuir* **2005**, *21*, 9231.
- (23) Henderson, D.; Gillespie, D.; Nagy, T.; Boda, D. *J. Chem. Phys.* **2005**, *122*, 084504.
- (24) Martín-Molina, A.; Quesada-Pérez, M.; Hidalgo-Álvarez, R. *J. Phys. Chem. B* **2006**, *110*, 1326.
- (25) Martín-Molina, A.; Maroto-Centeno, A.; Hidalgo-Álvarez, R.; Quesada-Pérez, M. *J. Chem. Phys.* **2006**, *125*, 144906.
- (26) Madurga, S.; Martín-Molina, A.; Vilaseca, E.; Mas, F.; Quesada-Pérez, M. *J. Chem. Phys.* **2007**, *126*, 234703.
- (27) Faraudo, J.; Travestet, A. *J. Phys. Chem. C* **2007**, *111*, 987.
- (28) Ibarra-Armenta, J. G.; Martín-Molina, A.; Quesada-Pérez, M. *Phys. Chem. Chem. Phys.* **2009**, *11*, 309.
- (29) Ottewill, R. H.; Shaw, J. N. *J. Colloid Interface Sci.* **1968**, *26*, 110.
- (30) Elimelech, M.; O'Melia, C. R. *Colloids Surf.* **1990**, *44*, 165.
- (31) Martín-Molina, A.; Quesada-Pérez, M.; Galisteo-González, F.; Hidalgo-Álvarez, R. *J. Phys. Chem. B* **2002**, *106*, 6881.
- (32) Quesada-Pérez, M.; Martín-Molina, A.; Galisteo-González, F.; Hidalgo-Álvarez, R. *Mol. Phys.* **2002**, *100*, 3029.
- (33) Martín-Molina, A.; Quesada-Pérez, M.; Galisteo-González, F.; Hidalgo-Álvarez, R. *J. Chem. Phys.* **2003**, *118*, 4183.
- (34) Martín-Molina, A.; Quesada-Pérez, M.; Galisteo-González, F.; Hidalgo-Álvarez, R. *Colloid Surf. A* **2003**, *222*, 155.
- (35) Martín-Molina, A.; Quesada-Pérez, M.; Galisteo-González, F.; Hidalgo-Álvarez, R. *J. Phys.: Condens. Matter* **2003**, *15*, S3475.
- (36) Quesada-Pérez, M.; González-Tovar, E.; Martín-Molina, A.; Lozada-Cassou, M.; Hidalgo-Álvarez, R. *Colloid Surf. A* **2005**, *267*, 24.
- (37) Lyklema, J.; Golub, T. *Croat. Chem. Acta* **2007**, *80*, 303.
- (38) Martín-Molina, A.; Maroto-Centeno, A.; Hidalgo-Álvarez, R.; Quesada-Pérez, M. *Colloid Surf. A* **2008**, *319*, 103.
- (39) Besteman, K.; Zevenbergen, M. A. G.; Heering, H. A.; Lemay, S. G. *Phys. Rev. Lett.* **2004**, *93*, 170802.

- (40) Besteman, K.; Zevenbergen, M. A. G.; Lemay, S. G. *Phys. Rev. E* **2005**, 72, 061501.
- (41) Besteman, K.; van Eijk, K.; Lemay, S. G. *Nature Phys.* **2007**, 3, 641.
- (42) Vaknin, D.; Kruger, P.; Losche, M. *Phys. Rev. Lett.* **2003**, 90, 178102.
- (43) Pittler, J.; Bu, W.; Vaknin, D.; Travesset, A.; McGillivray, D. J.; Lösche, M. *Phys. Rev. Lett.* **2006**, 97, 046102.
- (44) Jönsson, B.; Wenneström, H.; Halle, B. *J. Phys. Chem.* **1980**, 84, 2179.
- (45) Lekner, J. *Phys. A* **1991**, 176, 485.
- (46) Sperb, R. *Mol. Simul.* **1998**, 20, 179.
- (47) De Las Nieves, F. J.; Daniels, E. S.; El-Aasser, M. S. *Colloids Surf.* **1991**, 60, 107.
- (48) Bastos, D.; De Las Nieves, F. J. *Colloid Polym. Sci.* **1993**, 271, 870.
- (49) Miller, J. F.; Schätzel, K.; Vincent, B. *J. Colloid Interface Sci.* **1991**, 143, 532.
- (50) Mcneil-Watson, F.; Tscharnuter, W.; Miller, J. F. *Colloid Surf. A* **1998**, 140, 53.
- (51) Diehl, A.; Levin, Y. *J. Chem. Phys.* **2006**, 125, 054902.
- (52) Diehl, A.; Levin, Y. *J. Chem. Phys.* **2008**, 129, 124506.
- (53) Marcus, Y. *Ion Solvation*; John Wiley and Sons: Chichester, UK, 1985.
- (54) Israelachvili, J. *Intermolecular and Surface Forces*, 2nd ed.; Academic Press: London, 1992.
- (55) Lyklema, J. *Solid/liquid dispersions*; Academic Press: London, 1987.
- (56) Elimelech, M.; Gregory, J.; Jia, X.; Williams, R. *Particle Deposition & Aggregation. Measurement, Modelling and Simulation*; Butterworth Heinemann: Amsterdam, 1995.

JP900959Y